Electrochemistry Communications 162 (2024) 107705

Contents lists available at ScienceDirect

Electrochemistry Communications

journal homepage: www.elsevier.com/locate/elecom

Redox mediator interaction with *Cupriavidus necator* – spectroelectrochemical online analysis

André Gemünde [a], Jonas Gail [a], Dirk Holtmann [a,b,*]

[a] Institute of Bioprocess Engineering and Pharmaceutical Technology and Competence Centre for Sustainable Engineering and Environmental Systems, University of Applied Sciences Mittelhessen, 35390 Giessen, Germany
[b] Institute of Process Engineering in Life Sciences, Karlsruhe Institute of Technology, Kaiserstraße 12, 76131, Karlsruhe, Germany

ARTICLE INFO

Keywords:
Redox mediators
Anodic respiration
Cupriavidus necator
Parallelization
Bioelectrochemical system

ABSTRACT

Bioelectrochemical systems with *Cupriavidus necator* present a viable solution for harnessing H_2/CO_2 mixtures as substrates, employing mediated electron transfer to an infinite electron acceptor in the form of an anode instead of O_2. Fourteen redox mediators were spectroelectrochemically characterized, and their efficiency was evaluated through screening with *C. necator* in common cuvettes with screen printed electrodes (e-Cuvettes). Key performance indicators, including total turnover number, reduction rate, and growth, were analyzed. Ferricyanide emerged as highly effective for anodic respiration, reaching a total turnover number of 8.38 over 120 h of cultivation. On the other hand, phenazine methosulfate exhibited the highest reduction rate at 2.49 mM h^{-1} with a total of 5.16 turnovers. Contrary, growth impairment is reported for menadione, possibly leading to deficient anodic electron transfer. The utilization of a broad spectrum of these shuttle molecules highlights the potential for optimizing bioelectrochemical applications involving *C. necator*.

1. Introduction

A robust CO_2-utilizing strain capable of thriving on H_2 as an electron donor would be an ideal candidate for industrial fermentation of value-added products in the future. A promising microorganism to fulfil this task was found to be *Cupriavidus necator*. The conversion of H_2 as electron, and CO_2 as carbon source to products like the polymer alternative polyhydroxybutyrate [1] or terpenes for fragrance applications [2] is the key feature of *C. necator*. As genetic tools become more accessible, metabolic engineering facilitates the production of a broader array of products and applications [3,4].

However, challenges surface when O_2 is needed as the electron acceptor, particularly in large-scale reactors where the use of H_2/O_2 mixtures poses a significant explosion risk, which call for special precautions [5]. Bioelectrochemical systems offer a potential solution by replacing O_2 with an anode, circumventing safety concerns while at the same time overcoming oxygen transfer limitations and cost implications of transferring O_2 into the medium. Moreover, an anode serves as an inexhaustible electron acceptor, unlike gaseous or solid acceptors that necessitate replacement or regeneration [6,7].

Electron transfer mechanisms in this context involve direct contact with the electrode via redox-active proteins in the membranes, as well as via redox-active electron shuttles in the medium in a mediated electron transfer. Notably, *C. necator* lacks expression of redox-active proteins for maintaining a conductive "electron bridge" across the periplasmic space, necessitating the use of redox mediators (RMs) for efficient electron transfer to the anode.

The choice of RMs is critical and multifaceted, considering characteristics like membrane permeation (including hydrophobicity and charge), stability, toxicity, redox potential, solubility in aqueous media, and fast electron transfer [8,9]. Despite this, limited information exists regarding the interaction of *C. necator* with various redox mediators in so called "anodic respiration". Given that the process does not align with respiration in terms of generating a proton gradient through an electron transport chain, it should be emphasized that anodic respiration denotes the substitution of the terminal electron acceptor with the anode. Despite sporadic research efforts in this domain, a critical gap exists in the form of a mediator database specific to anodic respiration with

Abbreviations: BES, bioelectrochemical system; CV, cyclic voltammetry; DCIP, 2,6-dichloroindophenole; DHB, 3,4-dihydroxybenzaldehyde; FEC, ferricyanide; HNQ, 2-hydroxy-1,4-naphtaquinone; MB, methylene blue; MV, methyl viologen; PES, phenazine ethosulfate; PMS, phenazine methosulfate; RES, resorufin; RF, riboflavin; RM, redox mediator; RZ, resazurin; MEN, menadione; NR, neutral red; TTN, total turnover number.

* Corresponding author at: Institute of Process Engineering in Life Sciences, Karlsruhe Institute of Technology, Kaiserstraße 12, 76131 Karlsruhe, Germany.
E-mail address: dirk.holtmann@kit.edu (D. Holtmann).

https://doi.org/10.1016/j.elecom.2024.107705
Received 17 January 2024; Received in revised form 14 February 2024; Accepted 17 March 2024
Available online 18 March 2024

C. necator (and other organisms), underscoring the need for comprehensive exploration.

This study aims to address this gap by firstly, establishing a comprehensive dataset comprising crucial spectroelectrochemical data for diverse redox mediators, extending the scope of already existing data. Secondly, these RMs will be screened with *C. necator* for specific key performance indicators to determine their suitability for anodic respiration. By delving into the interaction dynamics between *C. necator* and various RMs, this research aims to pave the way for leveraging anodic respiration as a sustainable and efficient means of electron transfer, offering valuable insights for bioprocessing applications.

2. Materials and methods

2.1. Bacterial strains and chemicals

The strain *Cupriavidus necator* PHB$^-$4 [10] was employed in all biotic trials. Chemicals were sourced from Merck KGaA (Germany), VWR Chemicals (USA), Carl Roth GmbH & Co. KG (Germany), or Sigma Aldrich (USA).

2.2. Media and culture conditions

Cultures were incubated at 30 °C and 180 rpm in tubes containing 2.5 mL of LB medium (10 g L^{-1} tryptone, 5 g L^{-1} yeast extract, 10 g L^{-1} NaCl). For BES precultures, cryostocks were initially streaked on LB agar plates (15 g L^{-1} agar) and incubated overnight at 30 °C. Liquid precultures were subsequently generated by transferring a single colony into a 100 mL flask with baffles containing 20 mL of MMasy minimal medium [11] with 4 g L^{-1} fructose as carbon and electron source. The medium further contained 2.895 g L^{-1} Na_2HPO_4, 2.707 g L^{-1} $NaH_2PO_4{\cdot}H_2O$, 0.94 g L^{-1} $(NH_4)_2SO_4$, 0.8 g L^{-1} $MgSO_4{\cdot}7H_2O$, 0.097 g L^{-1} $CaSO_4{\cdot}2H_2O$, 0.17 g L^{-1} K_2SO_4, and 0.1 % (v/v) of trace element solution. The trace element stock solution consisted of 15 g L^{-1} $FeSO_4{\cdot}7H_2O$, 2.4 g L^{-1} $MnSO_4{\cdot}H_2O$, 2.4 g L^{-1} $ZnSO_4{\cdot}7H_2O$, 0.48 g L^{-1} $CuSO_4{\cdot}5H_2O$, 1.8 g L^{-1} $Na_2MoO_4{\cdot}2H_2O$, 1.5 g L^{-1} $Ni_2SO_4{\cdot}6H_2O$, and 0.04 g L^{-1} $CoSO_4{\cdot}7H_2O$ dissolved in 0.1 M HCl. Cultures were then incubated in an orbital shaker at 180 rpm (2.5 cm orbit, Multitron, Infors, Bottmingen, Switzerland).

2.3. Spectroelectrochemical mediator characterisation

Extinction characteristics of different mediators were determined by spectroelectrochemical analysis. Hereby, optical measurements are combined with cyclic voltammetry (CV) analysis. A spectroelectrochemical cell kit in a quartz cuvette was used (AKSTCKIT3, Pine Research Instrumentation Inc., USA). The electrode consisted of a gold working electrode with micro holes and a gold counter electrode on a ceramic substrate. A micro Ag/AgCl (3 M KCl) reference electrode (RRPEAGCL2, Pine Research Instrumentation Inc., USA) was immersed into the solution separately. The cell was heated to 30 °C and kept oxygen-free by sparging the headspace with N_2 (99.99 %). To eliminate any pH changes affecting the CV, measurements were carried out in 100 mM phosphate buffer (8.23 g L^{-1} Na_2HPO_4, 5.04 g L^{-1} NaH_2PO_4) at pH 7. Data was recorded on a Gamry Interface 1010B potentiostat (Gamry Instruments Inc., USA) at 50 and 10 mV s^{-1}. Each RM was used within a concentration range of 100 μM to 1 mM, if the solubility in aqueous buffer allowed. Poorly soluble mediators (such as menadione) were used at their maximum solubility.

2.4. BES screening

The screening device holds 8 independent 4 mL polystyrene cuvettes (Th. Geyer GmbH & Co. KG, Germany) in an automatic cuvette sampler within a spectrophotometer (Evolution 201, Thermo Scientific GmbH, Germany). Implementing screen-printed gold electrodes (C220 AT, Deutsche Metrohm GmbH & Co. KG, Germany) into each channel turns the cuvettes into an unseparated BES. For long term stability, the micro Ag/AgCl (3 M KCl) reference electrode was used again instead of the printed Ag pseudo electrode on the chip. Additionally, N_2 is sparged through the channels at a flow rate of 3.5 mL min^{-1} to keep the channels anaerobic and mixed. A detailed description of the device can be found in [12].

2.5. Electrochemical analysis and calculations

Cyclic voltammetry within the BES was carried out in using the screen-printed gold electrodes and Ag/AgCl (3 M KCl) reference electrodes. CVs were recorded at scan rates between 10 and 1000 mV s^{-1} at 30 °C without mixing the medium.

The midpoint potential (E_m) was derived as the mean of anodic and cathodic peak potentials obtained from CV analysis via the equation $E_m = (E_{ox} + E_{red})/2$. The total turnover number of the mediators (TTN) within the BES was calculated following a previously established method [13]. Reduction rates of redox mediators were determined by linear regression of the extinction values during the initial reduction of the respective mediator during BES cultivation. With calibration standards in the relevant concentrations of the mediator, the depleting or increasing linear extinction could be transformed into reduction rates in μM h^{-1}.

3. Results and discussion

3.1. Spectroelectrochemical redox mediator characterisation

A selection of fourteen RMs, each exhibiting different midpoint potentials (E_m) and featuring redox indicator properties (colour change upon reduction/oxidation), was chosen for assessment regarding their interaction with *C. necator* in a BES designed for anodic respiration (see Table 1). Via an online screening device based on cuvettes in an automatic sampler of a photometer, the redox state of each indicator RM can be monitored via a colour change upon reduction by *C. necator* at a characteristic wavelength (λ_c). This wavelength was determined by combining cyclic voltammetry with spectrophotometric analysis.

In total, during the experiment 3 oxidations and 3 reductions take

Table 1
E_m, ΔE, $I_{p,c}/I_{p,a}$, and λ_c of each RM measured by the described spectroelectrochemical approach. Conditions. 30 °C, anaerobic, pH 7, CV scan rate. 10 mV s^{-1}.

Redox mediator	E_m *vs.* Ag/AgCl (3 M KCl) [mV]	ΔE [mV]	$I_{p,c}/I_{p,a}$	λ_c [nm]
2,2′-azino-bis(3-ethylbenzothiazoline-6-sulfonic acid) (ABTS)	492	82	0.881	338/415
Methyl red (MR)	205.5	177	–	430
Ferricyanide (FEC)	194.6	315.1	0.925	320/420
3,4-dihydroxybenzaldehyde (DHB)	156.5	81	0.664	317
2,6-dichloroindophenole (DCIP)	16.3	66.5	0.889	607
Phenazine methosulfate (PMS)	−134.5	62	0.748	383
Phenazine ethosulfate (PES)	−144	68	0.682	383
Menadione (MEN)	−226.3	192.5	0.999	262/325
Resorufin (RES)	−242.3	51.5	1.037	568
Methylene blue (MB)	−261.5	63	1.024	642
2-hydroxy-1,4-naphtaquinone (HNQ)	−364.5	261	1.010	452
Riboflavin (RF)	−411	64	1.095	373/445
Neutral red (NR)	−553.5	73	1.575	445
Methyl viologen (MV)	−666.8	156.5	0.822	390/602

place (3 CV scans). Fig. 1 shows an example of how the λ_c of resazurin (RES) was determined via the aforementioned method. In Fig. 1 (a), the extinction spectra recorded over time create a 3-dimensional image of the redox reaction taking place at the working electrode during reduction and oxidation. For better visibility, Fig. 1 (b) depicts these spectra as a 2D topographic map. The repetitive redox reaction now enables to read off the λ_c and monitor side reactions. At the start of the CV scan at 400 mV (Fig. 1 (c)), meaning also 0 s in the extinction time-frame, distinct peaks at 270, 375 and 600 nm are visible. Now, as the potential is lowered (direction of the scan is shown with a red arrow) and the first reduction at −390 mV takes place, the extinction spectrum shifts to a single peak at 568 nm which rises and declines according to the reduction or oxidation occurring at the working electrode. Furthermore, the first reduction current appears to be much higher than in the second or third scan, indicating an irreversible reduction.

The observed phenomenon conforms to resazurin's characteristics, undergoing irreversible reduction to resorufin and resulting in a pink colour change. (Fig. 1 (d)) [14]. Resorufin can undergo a reversible redox reaction to dihydroresorufin in a two-electron transfer step. The colourless dihydroresorufin formation is evident through the extinction spectrum peak at 568 nm disappearing during reduction and the subsequent reappearance during resorufin formation at the working electrode (indicated with the black dashed line in Fig. 1 (b)). Therefore, λ_c can be determined with 568 nm, as this wavelength determines the redox state of the reversible electron transfer.

The same method was also applied to all 13 remaining RM to determine the λ_c. E_m for each RM for a single, reversible electron transfer reaction can also be obtained from the CVs. With this, both the reduction- and oxidation-potential can be determined and any following chemical reactions of the reactants are visible in peak current ratios ($I_{p,c}/I_{p,a}$) divergent from 1, since some of the reactant is now missing for the reverse reaction leading to a smaller peak current [15]. Furthermore, peak separation values (ΔE) can hint towards reversible or irreversible redox reactions of the RM, with a typical ΔE value close to 58 mV for a perfectly reversible one electron transfer process (at 25 °C). Fig. 2 shows all CVs obtained for 13 of the 14 RMs (except methyl red). For better visualisation, the obtained current values were normalized to equal values.

The determined E_m values as well as the $I_{p,c}/I_{p,a}$ ratios are listed in Table 1. Since a reaction can appear reversible at slower scan rates, these values are not universally valid [15]. In this case, a scan rate of 10 mV s^{-1} was applied. High ΔE values, especially higher than 58 mV under standard conditions, are a further indicator for quasi-reversible or irreversible reactions. For 2 electron transfer reactions, higher peak separations are to be expected, if one of the electron transfer steps is thermodynamically less favourable. However, above 140 mV both electron transfer steps should separate into single waves in the CV scan separation [16,17].

The CV of MR, depicted separately in Fig. 3, shows a typical irreversible behaviour within the wide potential range applied. For the first reversible electron transfer step, a potential of 140 to 165 mV is to be expected [18,19]. In this range, a smaller oxidation and reduction peak

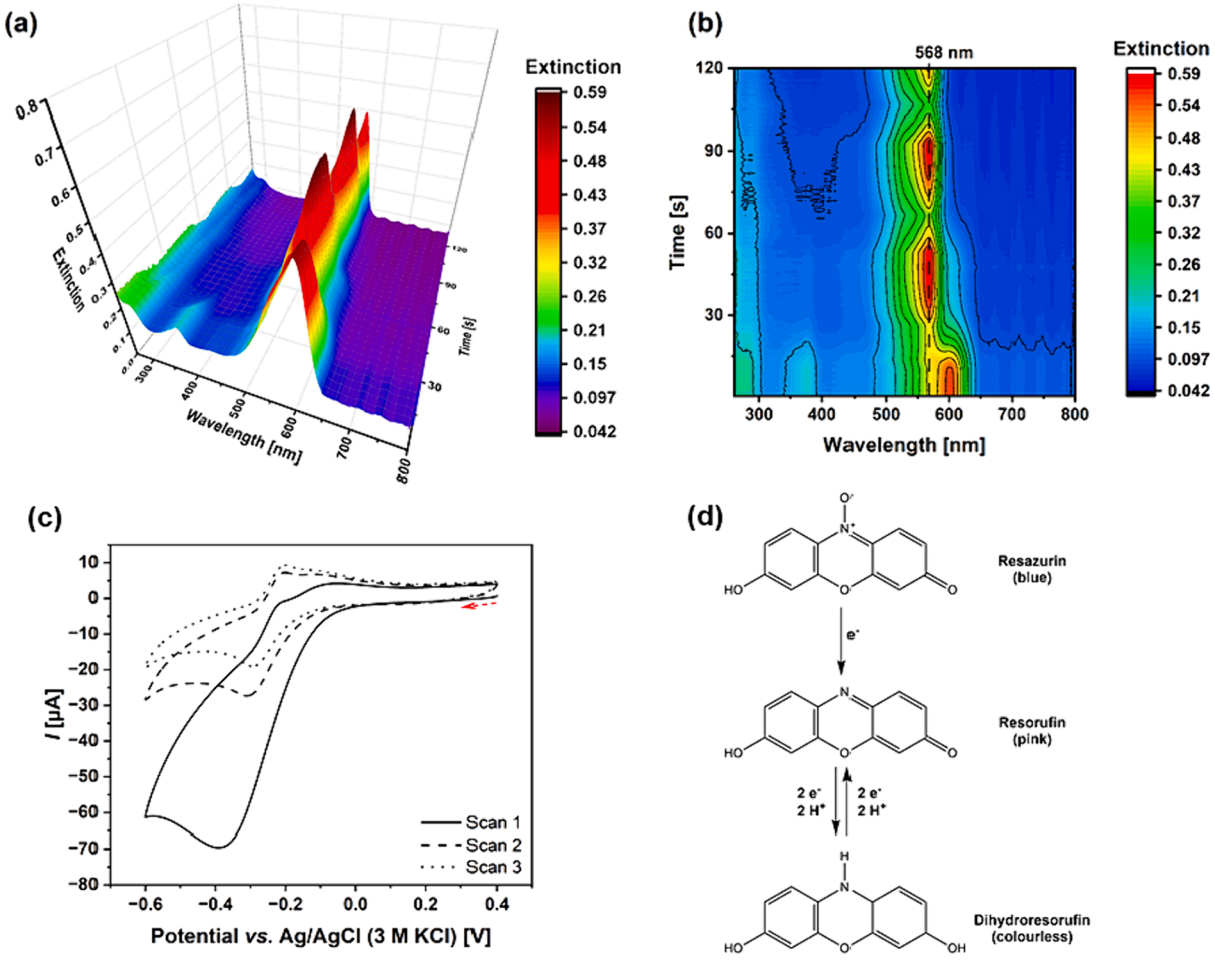

Fig. 1. Spectroelectrochemical characterisation of resazurin. (a) Extinction spectra over the course of 3 CV scans. (b) Topographical visualisation of the extinction spectra. (c) CV scans of 100 µM resazurin. Red arrow indicates the start of CV scan 1. Scan rate: 50 mV s^{-1}, 30 °C, anaerobic, pH 7. (d) Resazurin reaction scheme. Created with ChemDraw®.

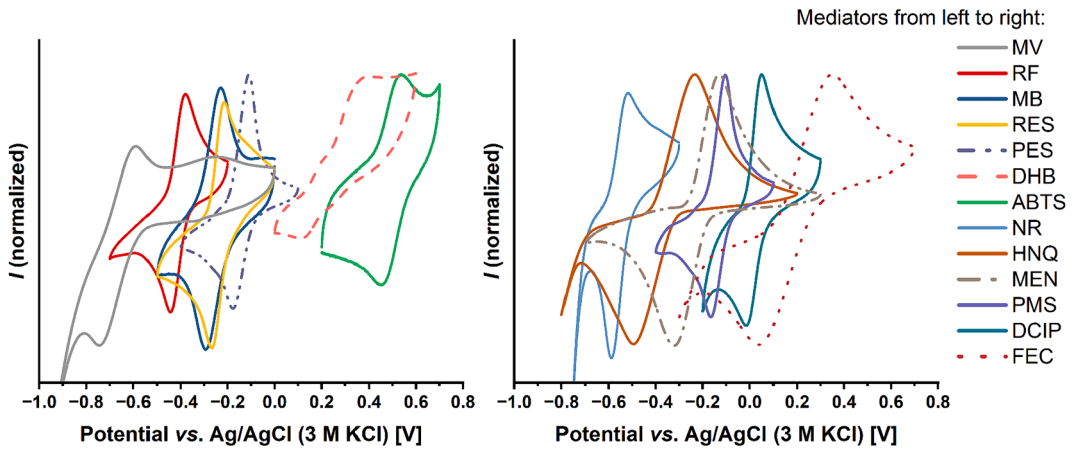

Fig. 2. CV scans of 13 redox mediators recorded with the spectroelectrochemical cell. Current values were normalized from 0 to 1 for better comparability of the mediators. Abbreviations: **MV:** methyl viologen, **RF:** riboflavin, **MB:** methylene blue, **RES:** resazurin, **PES:** phenazine ethosulfate, **DHB:** 3,4-dihydroxybenzaldehyde, **ABTS:** 2,2′-azino-bis(3-ethylbenzothiazoline-6-sulfonic acid, **NR:** neutral red, **HNQ:** 2-hydroxy-1,4-naphtaquinone, **MEN:** menadione, **PMS:** phenazine methosulfate, **DCIP:** 2,6-dichloroindophenole, **FEC.** ferricyanide. Conditions: 10 mV s^{-1}, 30 °C, anaerobic, pH 7.

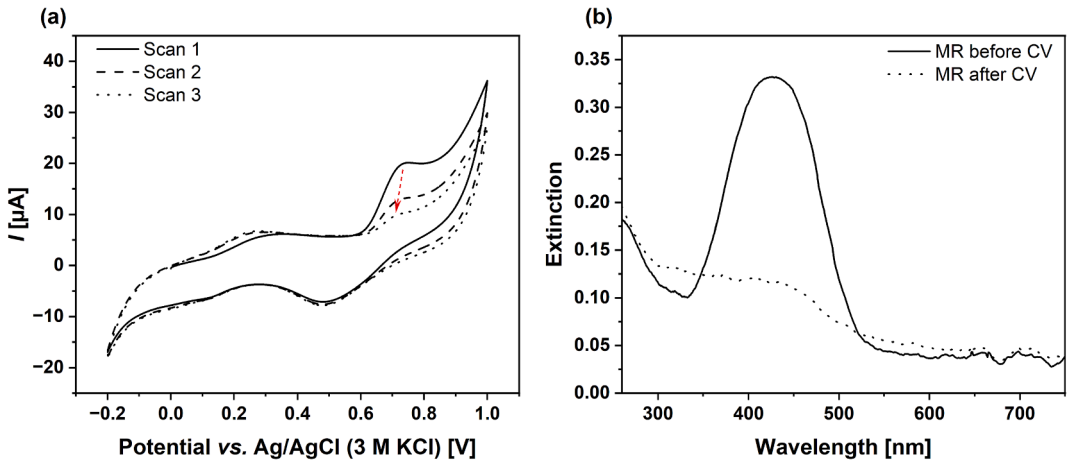

Fig. 3. (a) 3 CV scans of methyl red. The red arrow indicates the decrease in peak intensity over the course of the 3 scans. (b) Extinction spectrum taken before and after the CV scans. The vanished extinction maximum indicates an irreversible reaction took place. Scan rate. 50 mV s^{-1}, 30 °C, anaerobic, pH 7.

is visible in the CV scan. The oxidation potential of 294 mV and reduction potential of 117 mV result in E_m = 205.5 mV. However, a redox state characterisation by extinction measurement becomes impossible after MR is degraded above 700 mV [20]. The compound is therefore only applicable as a redox mediator below 700 mV. Side reactions like this could potentially degrade other mediators as well. However, within the potential ranges stated in Fig. 2, no such reaction was observed.

For all other RMs, Fig. 4 depicts the topographic view to determine each λ_c. The extinction spectrum of DHB did not exhibit a λ_c shift, possibly attributed to either a high scan rate, an inadequate concentration, or a slow electrochemical reaction. This phenomenon is also discernible in the minor peaks within the CV of DHB (Fig. 2). In the spectrum of MB, only one growing and decreasing peak is visible at 642 nm. The reasons for this might also be found within the electrochemical parameters. For MR and DHB, the maximum extinction from a separate spectrum was chosen as the λ_c for further biotic screening.

Table 1 summarizes the formal potentials and electrochemical peak separations calculated from CV scans and the λ_c determined from Fig. 4 for all examined RMs. In the case of MR, the reversible peaks were too small to determine the $I_{p,c}/I_{p,a}$ ratio accurately.

3.2. *In vivo* mediator interaction screening

Screening of the RMs was carried out in the e-Cuvette screening device, as already described elsewhere [12]. With this setup, the current density and the redox state of a RM can be determined online via the λ_c while simultaneously measuring OD_{600} for changes in cell density. Exemplarily, Fig. 5 illustrates a typical BES cultivation of *C. necator* in 6 parallel cuvettes and 2 abiotic controls with and without FEC. Prior to t_0 (abiotic phase), there is no evolution of current in the system. As soon as *C. necator* is introduced into the system at t_0, an anodic current starts to rise (magenta), while the FEC extinction at 420 nm (yellow dots) drops as it is reduced. Throughout cultivation, the anode partially re-oxidizes FEC, leading to an anodic current and an increase in extinction. After 118 h (t_1) the polarisation is stopped. The decline in extinction at 420 nm reaffirms that oxidized FEC remains present and is being reduced by viable cells.

The abiotic control including FEC polarized at 500 mV returns a steadily increasing current over time (Fig. 5 (a), dashed line), while FEC is also reduced as indicated by the declining extinction at 420 nm (Fig. 5 (b), yellow dots). It is most likely, that FEC is reduced at the cathode and simultaneously oxidized at the anode within this unseparated chamber (Fig. 5 (c)), while the cathodic reaction seems to be dominant and therefore shifts the ratio towards the reduced form. Other reactions, like

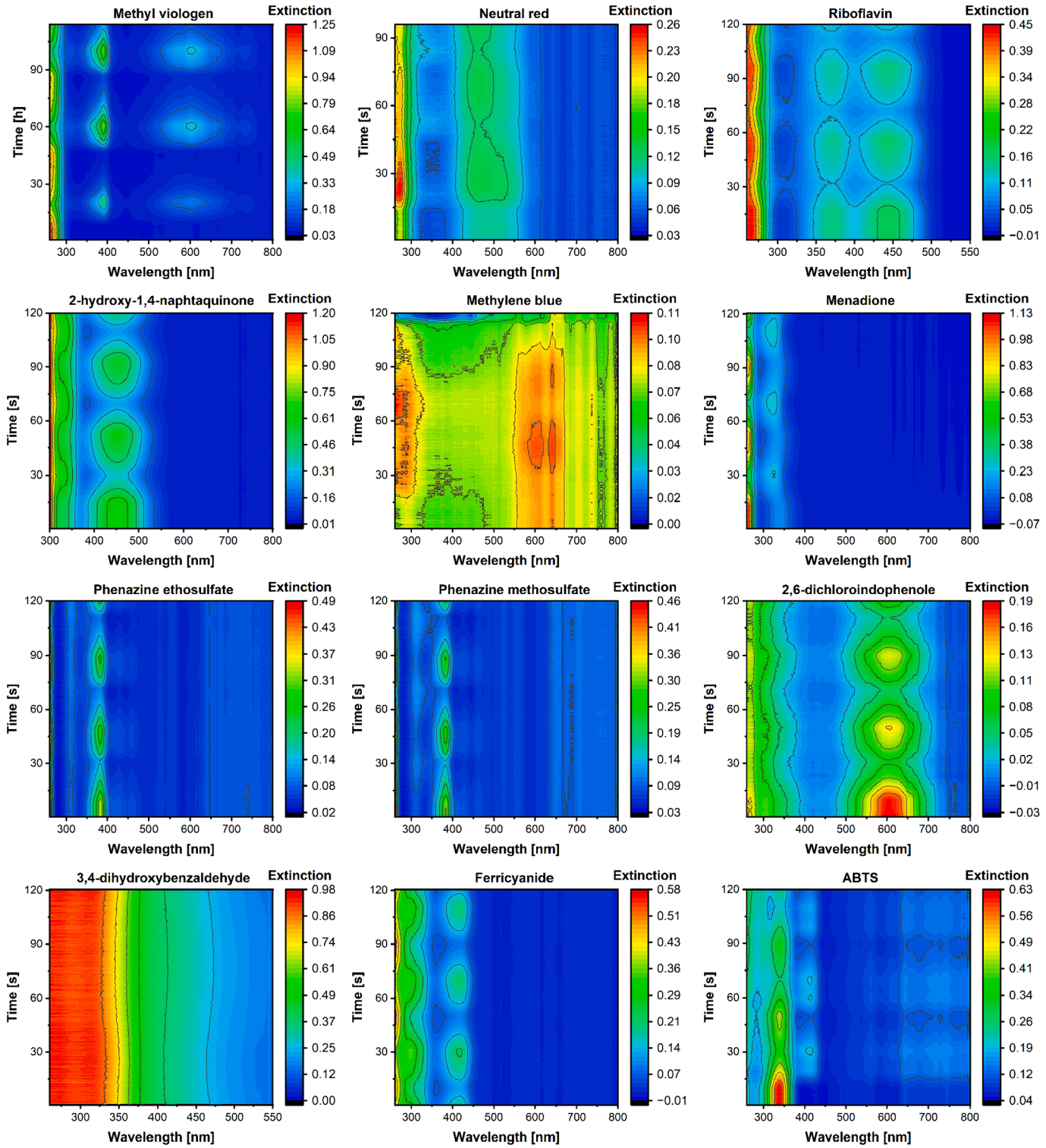

Fig. 4. Topographic visualization of the extinction spectra during 3 CV scans over the vertical time scale for each mediator used in this study (except MR and RES). The λ_c h of each mediator can be deduced from the recurring peaks over time. Conditions. 30 °C, anaerobic, pH 7, CV scan rate. 10 mV s^{-1}.

O_2 development (1.033 V *vs.* Ag/AgCl according to ΔG value) are not feasible at 500 mV and don't occur in CV analysis (Fig. 5 (d), dashed lines). Unknown side reactions from the medium can be observed within the CV. From the control cuvette without FEC, the direct involvement of these side reactions can be ruled out though, since the polarization of the pure medium doesn't result in a current evolving over time (Fig. 5 (a), dotted line).

The real-time analysis of current and extinction provides insights into three performance indicators, defining the efficiency of the mediator for anodic respiration. First, the slope of the extinction value during reduction of the RM enables reduction rate analysis. The reduction rate may indicate highly efficient mediators, regardless of the electrochemical regeneration system's efficiency. Second, with the charge transferred to the anode, the TTN can be calculated, giving further insight into the efficiency of the RM, independent of the concentration used. Moreover, the interaction between *C. necator* and a RM with a

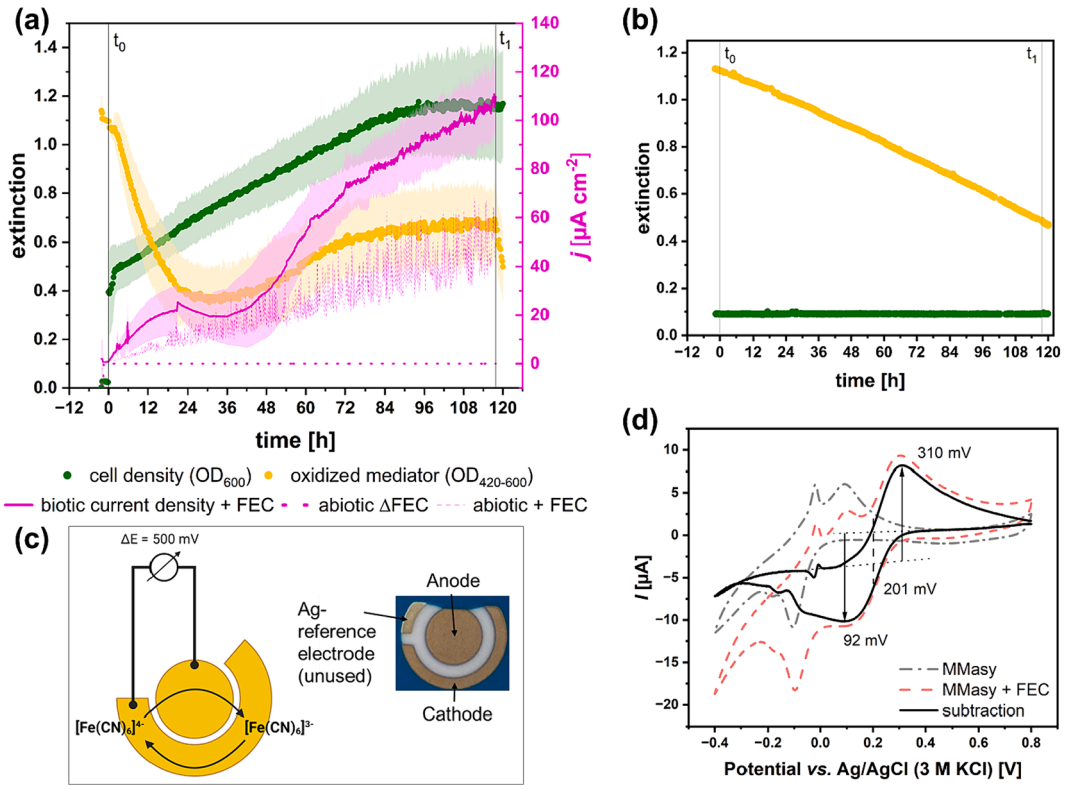

Fig. 5. (a) *C. necator* cultivation in e-Cuvettes with 1 mM FEC as redox mediator. t_0 marks the inoculation, while t_1 designates the point at which the polarisation is stopped. Current density (magenta) during polarisation at 500 mV for biotic cuvettes (solid line), abiotic control with FEC (dashed line), and without FEC (dotted line). Extinction values at 420 nm are plotted in yellow and cell density at 600 nm in green. (b) Abiotic control cuvette with FEC displays reduction of FEC, as indicated by the decline in OD_{420}. (c) Screen-printed electrode setup and abiotic redox cycle of FEC in the unseparated system. (d) CV scans of pure medium in comparison to medium with FEC in e-Cuvettes. Conditions. 3.5 mL MMasy medium, 30 °C, anaerobic, n = 6.

known redox potential provides insights into the minimum potential required for the oxidation of the yet unidentified interaction site(s) of *C. necator*. And third, growth rate analysis can hint towards impairments stemming from the redox mediator.

The described method was employed to screen all previously characterized RMs and evaluate their suitability for anodic respiration. Potentials for re-oxidation of the mediator were chosen above the oxidation potential of the RM, as determined by CV analysis. The first performance indicator, the reduction rate, is summarized in Table 2 including the applied concentrations and the observed growth rate. From the results, both phenazines, PMS and PES stand out with reduction rates of 2.49 and 0.25 mM h^{-1}, respectively.

Phenazine compounds are known for their high affinity towards the intracellular electron transfer chain. However, their stability within a BES varies between one and more than 10 days [21]. PMS decomposition to pyocyanine [22] also plays a role during the experiment. Abiotic controls of PMS at 300 mV exhibit a consistent decline in extinction at 383 nm with minimal current response, indicating both degradation and cathodic reduction. Moreover, the current density within the biotic cuvettes containing PMS never reaches a steady state, instead, it rapidly decreases after 2 h (Fig. 6 (a)).

The second performance indicator, the TTN, was determined over a 118 h cultivation period (Fig. 7). Interaction of the RM with *C. necator* is linked to the E_m of the respective RM and can reveal a minimum redox potential that is necessary for an electron shuttle compound to enable electron transfer from the still unknown interaction site(s) to the RM. By listing the TTN in a descending order according to their determined E_m, a major cut-off potential below –261 mV can be determined. However, HNQ is still interacting with *C. necator* in the first 10 h (data not shown), but the resulting current is extremely low resulting in a TTN of only 0.01. In conclusion, any mediator between 206 and −365 mV is able to interact with *C. necator*, indicating the interaction site(s) offer a broad potential range.

Table 2
RM reduction rates, concentrations, and observed growth rates of *C. necator* in BES cultivations.

RM	Concentration [µM]	Applied potential [mV *vs.* Ag/AgCl 3 M KCl]	Reduction rate [µM*h^{-1}]	Growth rate μ [h^{-1}]
ABTS	100	700	–	0.017
FEC	1000	500	49.43	0.015
DHB	120	700	3.73	0.013
MR	50	300	1.98	0.012
DCIP	80	300	35.3	0.009
PMS	50	300	2492.83	0.009
RES	100	0	99.85[a]	0.013
PES	50	300	245.15	0.011
MEN	50 % saturated solution	230	1.16[b]	0.003
MB	20	100	0.63	0.007
HNQ	400	100	–	0.007
RF	100	300	–	0.016
NR	100	−200	–	0.008
MV	625	−400	–	0.014
No RM				**0.011**

[a] only the initial reduction of RZ→RES was quantified in µM*h^{-1}
[b] measured in % h^{-1}

Upon comparing the TTN with the determined reduction rates, it becomes evident that slowly reduced redox mediators can still contribute to anodic respiration through consistent and stable cycling. E. g., MR is able to perform 4.2 cycles per molecule while only being reduced by *C. necator* at 1.98 µM h^{-1}. RES, on the other hand, is reduced

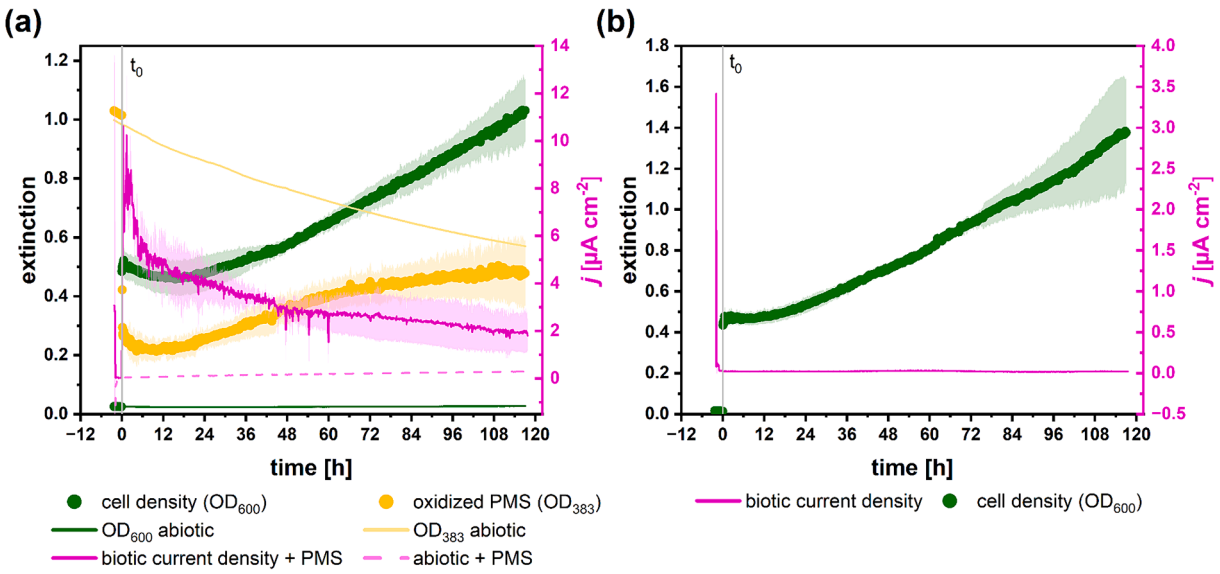

Fig. 6. (a) Current density of *C. necator* with 50 µM PMS in e-Cuvettes at 300 mV (magenta, n = 3) with extinction data (λ = 383 nm, yellow). Abiotic control with PMS at 300 mV (yellow line and magenta dashed line). (b) Control experiment with *C. necator* at 500 mV lacking a RM. Current density (magenta) and OD_{600} (green).

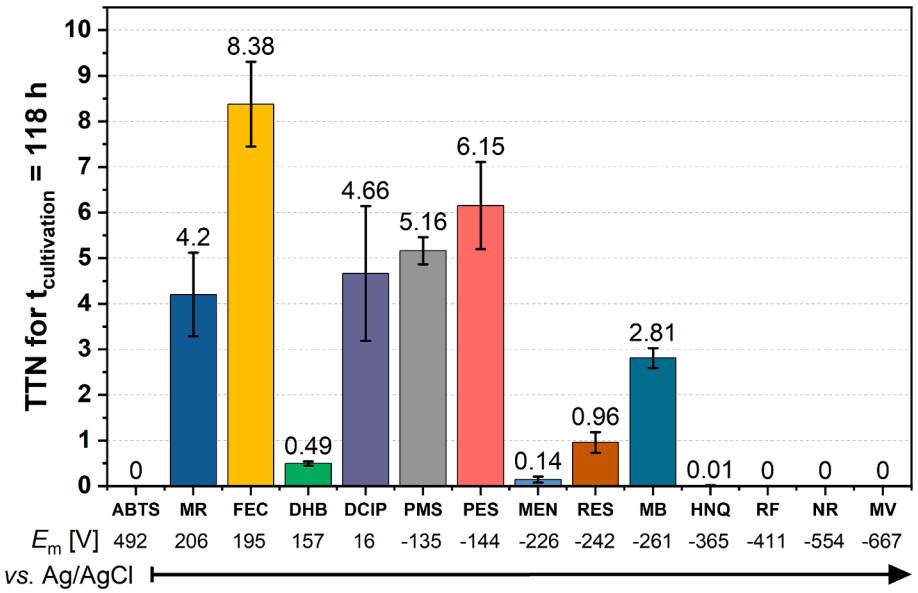

Fig. 7. TTN for all 14 RM in biotic electrochemical cultivations over 118 h with their respective redox potential *vs.* Ag/AgCl (3 M KCl). Conditions. 3.5 mL MMasy medium, 30 °C, anaerobic, n = 3. Error bars depict the standard deviation.

at 99.85 µM h^{-1} and only achieves 0.96 turnovers. As a lipophilic molecule, RES can most likely penetrate the cell membrane even though it is negatively charged [23]. This enables the direct oxidation of intracellular NADH, FADH or intracellular cytochromes. Transport within the bulk medium may limit the TTN and could hence benefit from a secondary, more hydrophilic redox mediator like FEC to facilitate electron transport to the anode. Furthermore, MR proves to be an effective RM with intact indicator properties in our BES when used at 300 mV *vs.* Ag/AgCl, were the molecule is not electrochemically degraded. MR, DCIP, PMS, PES, and FEC all resulted in a TTN above 4.2 promising future applications for anodic respiration. Both phenazines, MR, and DCIP share the hydrophobic characteristics with logP values of 3.06/2.9 for PES/PMS, 1.67 for MR, and 3.12 for DCIP [18,24]. FEC on the other hand, is more hydrophilic according to the logP value of −0.26 [18] and is most likely not membrane permeable due to the high negative charge. Hence, outer membrane porins likely play an important role in FEC transport. The affinity towards non-polar solvents is therefore not the key parameter for RM selection.

In a control experiment without a RM (Fig. 6 (b)), growth still occurs without the development of a current. Therefore, the growth is most likely caused by traces of O_2 entering the system as described before [12]. Comparing the growth rates with RMs from Table 2 to the reference rate without a RM, only MEN stands out with a significant inhibitory effect. This could also explain the exceptionally low TTN attributed to potential toxic effects on the metabolism. MB, HNQ, and NR have a slight inhibitory effect. Among them, only MB is deemed feasible for anodic respiration, with a TTN of 2.81.

4. Conclusions

In this study, λ_c and E_m values for 14 RMs were determined These values enable the online determination of redox states during BES

cultivation within a standard spectrophotometer. The determined ΔE and $I_{p,c}/I_{p,a}$ values CVs provided insights into which RM is capable of achieving reversible electron transfer with a gold electrode.

In BES screening experiments, phenazines proved to be highly efficient with maximum reduction rates of 2.49 mM h^{-1} and 0.25 mM h^{-1} for PMS/PES and a TTN of 5.16 and 6.15 respectively. Nevertheless, their stability constrains their applicability for long-term experiments. The screening further revealed that high reduction rates can occur independent of a high TTN. Especially FEC, delivering 8.38 turnovers while only being reduced at a rate of 49.43 μM h^{-1}, stands out in this context. The affinity towards organic solvents for each RM was termed secondary for selecting a RM, since both hydrophobic and hydrophilic RMs resulted in a similar TTN. However, to achieve an efficient process, the combination of both may lead to an optimal mediated electron transfer.

CRediT authorship contribution statement

André Gemünde: Writing – original draft, Visualization, Methodology, Investigation, Data curation. **Jonas Gail:** Investigation. **Dirk Holtmann:** Writing – review & editing, Supervision, Project administration, Funding acquisition, Conceptualization.

Declaration of competing interest

The authors declare that they have no known competing financial interests or personal relationships that could have appeared to influence the work reported in this paper.

Data availability

Data will be made available on request.

Acknowledgements and Funding

This work was created as part of the project “Bioelectrochemical and engineering fundamentals to establish electro-biotechnology for biosynthesis – Power to value-added products (eBiotech)”, which is funded by the Deutsche Forschungsgemeinschaft (DFG, German Research Foundation) – Project number 422694804.

References

[1] R.R. Dalsasso, F.A. Pavan, S.E. Bordignon, G.M.F. de Aragão, P. Poletto, Polyhydroxybutyrate (PHB) production by cupriavidus necator from sugarcane vinasse and molasses as mixed substrate, Process Biochem. 85 (2019) 12–18, https://doi.org/10.1016/j.procbio.2019.07.007.

[2] T. Krieg, A. Sydow, S. Faust, I. Huth, D. Holtmann, CO_2 to terpenes: autotrophic and electroautotrophic α-humulene production with cupriavidus necator, Angew. Chem. Int. Ed. Engl. 57 (2018) 1879–1882, https://doi.org/10.1002/anie.201711302.

[3] M. Ehsaan, J. Baker, K. Kovács, N. Malys, N.P. Minton, The pMTL70000 modular, plasmid vector series for strain engineering in cupriavidus necator H16, J. Microbiol. Meth. 189 (2021) 106323, https://doi.org/10.1016/j.mimet.2021.106323.

[4] J. Panich, B. Fong, S.W. Singer, Metabolic engineering of cupriavidus necator H16 for sustainable biofuels from CO_2, Trends Biotechnol. 39 (2021) 412–424, https://doi.org/10.1016/j.tibtech.2021.01.001.

[5] K. Tanaka, A. Ishizaki, T. Kanamaru, T. Kawano, Production of poly(D-3-hydroxybutyrate) from $CO_{(2)}$, $H_{(2)}$, and $O_{(2)}$ by high cell density autotrophic cultivation of alcaligenes eutrophus, Biotechnol. Bioeng. 45 (1995) 268–275, https://doi.org/10.1002/bit.260450312.

[6] I. Vassilev, G. Gießelmann, S.K. Schwechheimer, C. Wittmann, B. Virdis, J. O. Krömer, Anodic electro-fermentation: anaerobic production of L-lysine by recombinant corynebacterium glutamicum, Biotechnol. Bioeng. 115 (2018) 1499–1508, https://doi.org/10.1002/bit.26562.

[7] L. Gu, X. Xiao, S. Yup Lee, B. Lai, C. Solem, Superior anodic electro-fermentation by enhancing capacity for extracellular electron transfer, Bioresour. Technol. 389 (2023) 129813, https://doi.org/10.1016/j.biortech.2023.129813.

[8] M.L. Fultz, R.A. Durst, Mediator compounds for the electrochemical study of biological redox systems: a compilation, Anal. Chim. Acta 140 (1982) 1–18, https://doi.org/10.1016/S0003-2670(01)95447-9.

[9] Y. Yang, M. Xu, J. Guo, G. Sun, Bacterial extracellular electron transfer in bioelectrochemical systems, Process Biochem. 47 (2012) 1707–1714, https://doi.org/10.1016/j.procbio.2012.07.032.

[10] H.G. Schlegel, R. Lafferty, I. Krauss, The isolation of mutants not accumulating poly-beta-hydroxybutyric acid, Arch. Mikrobiol. 71 (1970) 283–294, https://doi.org/10.1007/BF00410161.

[11] A. Sydow, T. Krieg, R. Ulber, D. Holtmann, Growth medium and electrolyte-how to combine the different requirements on the reaction solution in bioelectrochemical systems using cupriavidus necator, Eng. Life Sci. 17 (2017) 781–791, https://doi.org/10.1002/elsc.201600252.

[12] A. Gemünde, J. Gail, J. Janek, D., Holtmann, e-Cuvettes parallelize electrochemical and photometric measurements in cuvettes and facilitate applications in bio-electrochemistry, Biosens. Bioelectron. X (2023) 100378, https://doi.org/10.1016/j.biosx.2023.100378.

[13] A. Gemünde, J. Gail, D. Holtmann, Anodic respiration of Vibrio natriegens in a bioelectrochemical system, ChemSusChem (2023) e202300181.

[14] R.S. Twigg, Oxidation-reduction aspects of resazurin, Nature 155 (1945) 401–402, https://doi.org/10.1038/155401a0.

[15] G.A. Mabbott, An introduction to cyclic voltammetry, J. Chem. Educ. 60 (1983) 697, https://doi.org/10.1021/ed060p697.

[16] E.S. Da Barreto, B.E.L. Baêta, M.C. Pereira, D. Pasquini, V.M. Guimarães, L.V. A. Gurgel, 2-Hydroxy-1,4-naphthoquinone (lawsone) as a redox catalyst for the improvement of the alkaline pretreatment of Sugarcane bagasse, Energy Fuels 34 (2020) 16228–16239, https://doi.org/10.1021/acs.energyfuels.0c02990.

[17] N. Elgrishi, K.J. Rountree, B.D. McCarthy, E.S. Rountree, T.T. Eisenhart, J. L. Dempsey, A Practical beginner’s guide to cyclic voltammetry, J. Chem. Educ. 95 (2018) 197–206, https://doi.org/10.1021/acs.jchemed.7b00361.

[18] F.J. Rawson, A.J. Downard, K.H. Baronian, Electrochemical detection of intracellular and cell membrane redox systems in Saccharomyces cerevisiae, Sci. Rep. 4 (2014) 5216, https://doi.org/10.1038/srep05216.

[19] D. Kul, G. Öztürk, Poly(Methyl red) modified glassy carbon electrodes: electrosynthesis, characterization, and sensor behavior, Electroanalysis 29 (2017) 1721–1730, https://doi.org/10.1002/elan.201700043.

[20] C.C.d.O. Morais, A.J.C. Da Silva, M.B. Ferreira, D.M. de Araújo, C.L.P.S. Zanta, S.S. L. Castro, Electrochemical degradation of methyl red using $Ti/Ru_{0.3}Ti_{0.7}O_2$: fragmentation of azo group, Electrocatalysis 4 (2013) 312–319, https://doi.org/10.1007/s12678-013-0166-x.

[21] A. Chukwubuikem, C. Berger, A. Mady, M.A. Rosenbaum, Role of phenazine-enzyme physiology for current generation in a bioelectrochemical system, Microb. Biotechnol. (2021).

[22] B. Jahn, N.S.W. Jonasson, H. Hu, H. Singer, A. Pol, N.M. Good, H.J.M.O. den Camp, N.C. Martinez-Gomez, L.J. Daumann, Understanding the chemistry of the artificial electron acceptors PES, PMS, DCPIP and Wurster’s blue in methanol dehydrogenase assays, J. Biol. Inorg. Chem. 25 (2020) 199–212, https://doi.org/10.1007/s00775-020-01752-9.

[23] J.L. Chen, T.W.J. Steele, D.C. Stuckey, Metabolic reduction of resazurin; location within the cell for cytotoxicity assays, Biotechnol. Bioeng. 115 (2018) 351–358, https://doi.org/10.1002/bit.26475.

[24] M. Surmeian, A. Hibara, M. Slyadnev, K. Uchiyama, H. Hisamoto, T. Kitamori, Distribution of methyl red on the water-organic liquid Interface in a microchannel, Anal. Lett. 34 (2001) 1421–1429, https://doi.org/10.1081/AL-100104916.